Received: 2 July 2019 | Revised: 23 January 2020 | Accepted: 23 January 2020

DOI: 10.1002/bit.27286

ARTICLE

BIOTECHNOLOGY BIOENGINEERING WILEY

Processing two environmental chemical signals with a synthetic genetic IMPLY gate, a 2-input-2-output integrated logic circuit, and a process pipeline to optimize its systems chemistry in *Escherichia coli*

Sayak Mukhopadhyay | Kathakali Sarkar | Rajkamal Srivastava | Arijit Pal | Sangram Bagh

Biophysics and Structural Genomics Division, Saha Institute of Nuclear Physics, Homi Bhabha National Institute (HBNI), Kolkata, India

Correspondence
Sangram Bagh, Biophysics and Structural Genomics Division, Saha Institute of Nuclear Physics, Homi Bhabha National Institute (HBNI), Kolkata, West Bengal 700064, India.
Email: sangram.bagh@saha.ac.in

Funding information
Department of Atomic Energy, Government of India, Grant/Award Number: SINP Intramural Funding; Department of Science and Technology, Ministry of Science and Technology, Grant/Award Number: Ramanujan Fellowship; BIRAC, Grant/Award Number: Synthetic Biology

Abstract

Synthetic genetic devices can perform molecular computation in living bacteria, which may sense more than one environmental chemical signal, perform complex signal processing in a human-designed way, and respond in a logical manner. IMPLY is one of the four fundamental logic functions and unlike others, it is an "IF-THEN" constraint-based logic. By adopting physical hierarchy of electronics in the realm of in-cell systems chemistry, a full-spectrum transcriptional cascaded synthetic genetic IMPLY gate, which senses and integrates two environmental chemical signals, is designed, fabricated, and optimized in a single *Escherichia coli* cell. This IMPLY gate is successfully integrated into a 2-input-2-output integrated logic circuit and showed higher signal-decoding efficiency. Further, we showed simple application of those devices by integrating them with an inherent cellular process, where we controlled the cell morphology and color in a logical manner. To fabricate and optimize the genetic devices, a new process pipeline named NETWORK Brick is developed. This pipeline allows fast parallel kinetic optimization and reduction in the unwanted kinetic influence of one DNA module over another. A mathematical model is developed and it shows that response of the genetic devices are digital-like and are mathematically predictable. This single-cell IMPLY gate provides the fundamental constraint-based logic and completes the in-cell molecular logic processing toolbox. The work has significance in the smart biosensor, artificial in-cell molecular computation, synthetic biology, and microbiorobotics.

KEYWORDS
genetic device, logic gates, molecular computation, synthetic biology, synthetic gene circuit

1 | INTRODUCTION

The ability to compute the environmental chemical signals by bacteria with synthetic molecular genetic devices is paving the way of advanced molecular computation, future smart biosensors, microbiorobotics, and their numerous applications (Andrianantoandro, Basu, Karig, & Weiss, 2006, Ashkenasy, Hermans, Otto, & Taylor, 2017; Goñi-Moreno & Nikel, 2019; Kim, Steager, & Agung, 2012). The basic logic processing including NOT, BUFFER, AND, OR, NAND, NOR, XOR, and XNOR has been demonstrated in living bacterial cells and in the last 15 years, various designs and implementation strategies for almost all logic gates have been realized (Bonnet, Yin,

Ortiz, Subsoontorn, & Endy, 2013; Green et al., 2017; Jusiak, Cleto, Perez-Piñera, & Lu, 2016; Moon, Lou, Tamsir, Stanton, & Voigt, 2012; Nomura & Yokobayashi, 2015; Siuti, Yazbek, & Lu, 2013). Here, the inputs are environmental chemical signals, which are sensed, integrated, and computed inside cells by various molecular modalities including transcription factors, recombinases, CRISPRi/dCas9, RNA, and ribozymes and produced output by expressing proteins, nucleic acids, or metabolites (Bonnet et al., 2013; Green et al., 2017; Jusiak et al., 2016; Moon et al., 2012; Nomura & Yokobayashi, 2015; Siuti et al., 2013).

IMPLY is one of the most fundamental four logic functions (AND, OR, NOT, and IMPLY), which were proposed in 1910 by Whitehead and Russell in *Principia Mathemetica* (Russell & Whitehead, 1910). Unlike the other three logic functions, IMPLY is a constraint-based logic and is defined by its theorem as, "If "P" is TRUE then output follows "Q" otherwise it is TRUE" (Borghetti et al., 2010; Russell & Whitehead, 1910). IMPLY has applications in robotics, control systems, and artificial intelligence (Borghetti et al., 2010; Castelfranchi & Lespéran, 2001; Kampis, 1991; Swart, & Nederpelt, 1992). In principle, any circuit can be made from universal NOR or NAND gates. However, from a practical point of view, it is not always the case. For example, to create an IMPLY function, three NOT gates are required. Therefore, the application of IMPLY gates is more useful for circuits like decoder or adder, instead of IMPLY equivalent three NOR gates. This is specifically important for creating large and complex synthetic genetic circuits, where an increasing number of genetic components and cascaded steps often hinder the correct functionality of the circuits.

An IMPLY type behavior in bacterium, was reported before (Weiss & Basu, 2002; Yokobayashi, Weiss, & Arnold, 2002), where only one environmental chemical (isopropyl β-D-1-thiogalactopyranoside [IPTG]) signal was sensed and processed, whereas the other input was a constitutively expressed intracellular protein (lacI; Weiss & Basu, 2002; Yokobayashi et al., 2002). This intracellular input protein (lacI) was always present in a high amount (input logic level 1) and thus it cannot be brought to logic level "0" (Weiss & Basu, 2002; Yokobayashi et al., 2002). As a result, the 0,0 and 1,0 input logic levels, with respect to IPTG and lacI, respectively, could not be realized. Further, IPTG and lacI cannot be treated as independent inputs as the function of lacI depends on IPTG. Thus it cannot be used as a full-spectrum chemical signal processing IMPLY device for two environmental chemical signals. Full-spectrum IMPLY gates were constructed by combing multiple NOR gates by engineering bacterial communications, where three different cell populations were required to construct the IMPLY gates (Tamsir, Tabor, & Voigt, 2011). N-IMPLY (inverted output of IMPLY) gate was reported in bacterial and mammalian cells (Ausländer, Ausländer, Müller, Wieland, & Fussenegger, 2012; Guet, Elowitz, Hsing, & Leibler, 2002). Further, using a serine recombinase-based system, IMPLY gates were constructed in single *Escherichia coli* cells (Siuti et al., 2013). Depending on the orientation, each recombinase targets its related recognition sites to invert or excise DNA. This strategy does not need the cascaded transcription regulations, a conventional way to design and fabricate synthetic genetic logic gates. However, recombinase-based circuit comes with memory and is irreversible in nature. In the presence of inputs, the circuit goes to the ON state and cannot come back to OFF state even the inputs are withdrawn. Although this clever design has important applications in state-dependent circuits, it cannot be used to develop combinational circuits, which depend on the input values at a given instance.

Here, by adapting the electronics hierarchy (cascaded) principle, we designed, fabricated, characterized, and optimized a 2-input fully chemically controllable molecular genetic IMPLY gate in living single *E. coli*. The engineered *E. coli* can sense and process two environmental chemical signals and produce a fluorescent output by expressing a fluorescent protein following the IMPLY logic function. Our design is based on cascaded transcriptional regulation. The system is memoryless and reversible. Further, following the same cascaded principle, we created and tested an integrated 2-input-2-output genetic circuits by cascading the IMPLY gate. As such transcriptional circuit requires several bioparts in harmony, one of the fundamental challenges to make such circuit works is the optimization of various molecular genetic parts, such that they work together as a functional device. To fabricate the circuit and optimize its systems chemistry inside a cell, we developed a new process pipeline, named NETWORK brick, for systematic fabrication, fast kinetic optimization, and elimination of unwanted kinetic influence from one set of biochemical modules to other. A simple mathematical model captures the essential features of the device at the steady state. We showed that those circuits are digital as well as mathematically predictive.

2 | MATERIALS AND METHODS

2.1 | Promoters, primers, genes, plasmids, and bacterial cell strains

The step-by-step process of fabrication of the genetic circuits using NETWORK brick, the new process pipeline we developed (see Section 3 for details), is shown in Table S1. The full lists of plasmids, primers, and ribosome binding sites (RBSs) are shown in Tables S2–S4, respectively. All empty vectors were made by incorporating double-stranded DNA fragments according to our designed framework with appropriate restriction sites in two backbone plasmids—pOR-EGFP-12 and pOR-Luc-31 (a gift from Prof. David McMillen, University of Toronto, Toronto, Canada). The DNA fragments were synthesized from Invitrogen. The required genes and promoters are PCRed with appropriate primers (Table S3) and incorporated accordingly in the empty plasmids (Table S2). The NETWORK Brick pipeline was followed to make the logic circuits as shown in Table S1. Polymerase chain reactions (PCRs) were performed using KOD hot-start DNA polymerase (Merck Millipore) and primers were synthesized from Integrated DNA Technologies, Singapore. The bioparts were assembled into the NETWORK brick plasmid vectors using sticky end ligation as generated according to the NETWORK brick principle (Figure 2). Plasmids were transformed in chemically competent DH5αZ1 *E. coli* strains (Table S1). Sequencing of the plasmids was done from Eurofins Genomics India Pvt Ltd.,

Bangalore, India. Restriction endonuclease and T4 DNA ligase were bought from New England BioLabs; plasmid isolation, gel extraction, and PCR purification kits were from Qiagen.

2.2 | Cell growth for genetic constructs characterization

Cells from overnight culture in Luria–Bertani (LB) media with appropriate antibiotics (100 μg/ml and 34 μg/ml for ampicillin, and chloramphenicol, respectively) were diluted 100 times in fresh LB media with antibiotics and inducers IPTG (0 and 10 mM) or aTc (0 ng/ml of aTc and 200 ng/ml; Sigma Aldrich) as appropriate. It was grown for 10 hr at 37°C, ~ 250 rpm followed by dilution in fresh media, regrown for another 6 hr at 37°C, ~ 250 rpm before measurements.

2.3 | Fluorescence and optical density measurements

Cells were washed two times and diluted in phosphate buffered saline (PBS; pH around 7.4) and loaded onto a 96-well black microtiter plate (Greiner Bio-One). The fluorescence was measured in a Synergy HTX Multi-Mode reader (Biotek Instruments). For enhanced green fluorescent protein (EGFP) and *TdTomato*, the cells were excited with a white light passed through excitation filters 485/20 nm and 540/35 nm, respectively, and emission was passed through 516/20 and 590/20 nm bandpass filters, respectively. The optical density (OD) of the cell samples was measured as OD600. First, OD normalized value of raw fluorescence data was calculated by dividing raw fluorescence values with respective OD600. Similarly, OD normalized autofluorescence was measured with cells without the plasmids divided by respective OD600. Next, we subtracted the OD normalized autofluorescence from the OD normalized fluorescence to get a single experiment normalized fluorescence value for each experiment. Average normalized fluorescence for each data point (each specific induced or uninduced condition) was determined by averaging single experiment normalized fluorescent values over a minimum of three biological replicates. For a set of experiment, the highest average normalized fluorescence value obtained at a specific data point (e.g., in presence of both ATC and IPTG) within the set of experiments (i.e., experiments with combination of ATC and IPTG) was taken as 1 and all other average normalized fluorescence values within that specific set of experiment were scaled accordingly. These scaled values were denoted as normalized fluorescence (a.u.) in the figures. For the 3D input-output relationship experiments, single biological replicate was characterized. Here, both IPTG and ATC concentrations were varied simultaneously and EGFP and *TdTomato* expression were measured against around 130 different IPTG and ATC concentration points, which are different than the ATC/IPTG concentration in dose-response curves.

2.4 | Mathematical modeling, data fitting, and simulation

Details of the mathematical modeling, data fitting, and simulation can be found in Note S1 in Supporting Information Material.

2.5 | Microscopy

The bacterial cells were harvested at 4,000 rpm, washed, and finally diluted in PBS (pH = 7.4). To visualize, the cell suspension was put onto a 1% thin agarose pad (SeaKem LE agarose) and was covered with a cover slip. The differential interference contrast (DIC) and fluorescence imaging were performed in Zeiss LSM 710 confocal microscope in the epifluorescence mode, keeping the pin-hole completely open. The cells expressing EGFP were excited using 488-nm laser and fluorescence was collected through appropriate dichroic and filters sets for EGFP. The DIC images were taken using a DIC attachment. The images were captured and postprocessed using Zen 2009 software.

3 | RESULTS AND DISCUSSION

3.1 | Design of IMPLY logic for sensing and processing two extracellular environmental chemicals

The design and experimental behavior of the IMPLY gate is shown in Figure 1. The electronic equivalence (Figure 1a) of the molecular design (Figure 1b) is based on modular DNA-parts and their specific interactions with transcription factors and RNA polymerase. One EGFP gene (output) was placed under a synthetic hybrid promoter P_{LTATAA} (Sarkar, Mukhopadhyay, Bonnerjee, Srivastava, & Bagh, 2019). The promoter P_{LTATAA} worked in such a way that lac repressor (LacI) or Tet repressor (tetR) proteins could bind and inhibit its function. Small molecule inducers IPTG and anhydrotetracycline (ATC) were sensed and interacted allosterically with LacI and tetR, respectively, and made a conformational change (Lutz & Bujard, 1997), which could no longer inhibit the promoter P_{LTATAA}. Another EGFP gene was placed under P_R promoter, which got inhibited by a mutated version of a lambda repressor CI protein (CIm) (Sarkar et al., 2019). The CIm gene was under the control of ATC inducible PLtetO-1 promoter (Sarkar et al., 2019). The design is generic and can be used to create IMPLY gates, which may sense and process other environmental signals. The fabrication of the design and its optimization (see Section 3.2) showed imperfect (Figure 1c) and matching (Figure 1d) behavior. The details can be found in Section 3.3.

3.2 | NETWORK brick: A strategy for construction and kinetic optimization of gene circuits

The successful engineering of an artificial molecular genetic device depends on the kinetic match among multiple reactions and

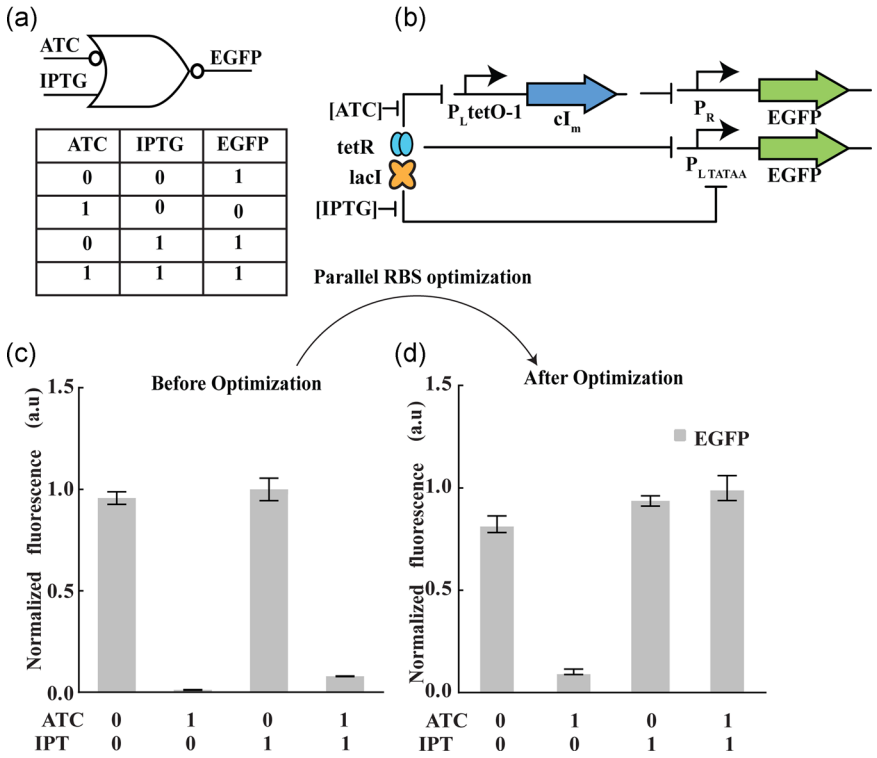

FIGURE 1 Design and testing of molecular IMPLY gate. (a) Electronic equivalent representation and truth table. (b) Biomolecular design. (c) Experimental behavior before optimization and (d) experimental behavior after optimization [Color figure can be viewed at wileyonlinelibrary.com]

interactions between various DNA modules within the circuit. The fabrication of the proposed design needs a process pipeline for assembly of multiple DNA cassettes, fast optimization of the rate of gene expression, and reduction of unwanted kinetic influence. Here, DNA cassette is defined as "promoter-RBS-gene-transcription terminator" sequences, where each of the nonreducible DNA entities like promoter or RBS is defined as DNA-parts. The gold standard for such assembly is "biobrick" assembly method and their modified schemes (Anderson, Voigt, & Arkin, 2007; Cameron, Bashor, & Collins, 2014; Che, 2004; Phillips & Silver, 2006; Shetty, Endy, & Knight, 2008). However, applying those strategies to optimize the kinetics of gene expression by altering RBS within an assembled cassette is not possible. This is due to the fact that the assembled cassette from biobrick principle does not have any restriction site within bioparts (Anderson et al., 2007; Shetty et al., 2008). Second, in biobrick strategy, two cassettes can only be assembled in a single direction. This unidirectionality results in a nonzero influence of a strong promoter in the upstream cassette on the kinetics of gene expression of the downstream cassette, even in the presence of transcription terminator (Chen et al., 2013).

To address this gap and fabricate our design, we first developed an easy, systematic, and faster assembly and optimization pipeline and named it as NETWORK brick (Figure 2). It consists of two plasmid vectors (~20–30 nm; Fink et al., 2006) named as forward cassette empty vector (FCEV) and reverse cassette empty vector (RCEV). In NETWORK brick, within a single DNA cassette, each DNA -part was flanked with two unique restriction sites. Thus, any of the DNA-parts could be replaced for optimization by a library of modified DNA parts in parallel without starting from scratch (Figure 2a). Next, biobrick type prefix (PstI, BamHI) and suffix (BglI, SalI) restriction sites were introduced upstream and downstream of a DNA cassette, respectively (Figure 2a). This allowed assembling multiple cassettes together into a single direction using only those four enzymes (Figure 2b) by isocaudomeric principle (Shetty et al., 2008). A second plasmid system, named as reverse cassette empty vector (RCEV), was created (Figure 2c). In RCEV, positions of the first and last restriction sites of the cassette (XhO-I and AvrII, respectively) were swapped, such that if a cassette from FCEV was incorporated in RCEV, the 5′-3′ sequence direction of the cassette would be changed. Thus assembling this reverse cassette from RCEV with forward cassette in FCEV resulted in the two cassettes in the opposite direction (Figure 2c). Thus NETWORK brick system would allow integrating multiple DNA cassettes in any direction and parallel optimization of a DNA-biopart within a cassette. Here, we showed a comparison between NETWORK brick and biobrick for constructing, assembling, and optimization of two genetic cassettes (Table S4). A detailed step-by-step process pipeline of NETWORK brick for constructing IMPLY gates and other gates (Section 3.3) is already shown in Table S1.

3.3 | Construction, characterization and optimization of IMPLY gate

Using this NETWORK brick pipeline, we first constructed the IMPLY gate in a plasmid and transformed into *E. coli* DH5αZ1 cell strain (Table S1), which constitutively produced TetR and LacI proteins

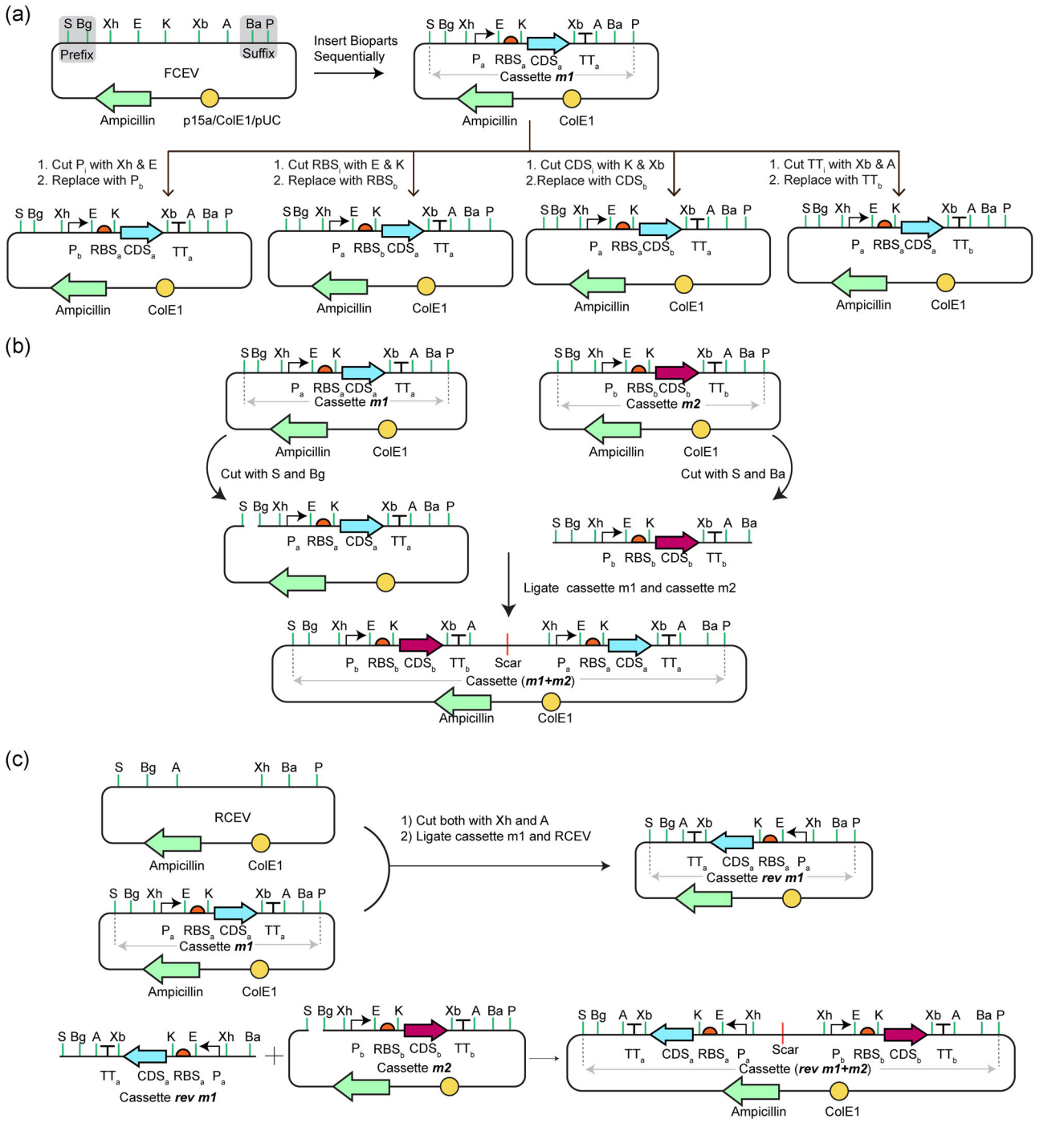

FIGURE 2 NETWORK Brick, the new biochemical process pipeline. (a) Forward cassette empty vector (FCEV) with its restriction sites. The biobrick type prefix and suffix consist SalI (S), BglII (Bg) and BamHI (Ba), PstI (P) respectively. The empty cassette consist XhO-I (Xh), EcorI (E), KpnI (K), XbaI (Xb), and AvrII (A). P, RBS, CDS, and TT represent promoter, ribosome binding site, gene, and transcription terminator DNA sequences, respectively. The process pipeline of inserting individual biopart(s) in FCEV is also shown. (b) Process pipeline for assembling two genetic cassettes in a single direction. (c) Schematic of reverse cassette empty vector and process pipeline for assembling two genetic cassettes in two opposite directions [Color figure can be viewed at wileyonlinelibrary.com]

(Lutz & Bujard, 1997) (experimental section; Tables S1–S3). Next, cells were grown in appropriate condition (experimental section) and experimental characterization of IMPLY logic circuit was performed in the absence or presence of input chemical signals, ATC (0 and 200 ng/mL) and IPTG (0 and 10 mM). The EGFP fluorescence was measured as a logic output. The experimental behavior was plotted in Figure 1c, which showed an imperfect behavior for an IMPLY gate.

Failure analysis on this device suggested that the sensing of the two environmental chemicals worked. However, during the signal processing, the gene expression rate of output EGFP from P_R

promoter was much higher than the hybrid promoter P_{LTATAA} (Figure S1). Therefore, one of the crucial design criteria was to reduce the EGFP formation rate from the P_R promoter to match the expression from the hybrid promoter P_{LTATAA}. The NETWORK brick pipeline, in this study, was developed to meet such challenges in the fabrication line by allowing easy optimization. In this direction, we designed seven new RBSs and estimated their relative strength using thermodynamic calculation (RBS calculator; Espah Borujeni, Channarasappa, & Salis, 2014; Salis, Mirsky, & Voigt, 2009). Applying NETWORK brick, we replaced the RBS between P_R promoter and EGFP gene of the cassette 5 (Table S1), a constituent cassette of the IMPLY gate, with seven different RBSs of varying strength (Table S5) in parallel. The resulting cassettes were named as cassette 9i1 to 9i7. IMPLY gate circuits containing cassette 9i2 and 9i4, which contains RBS-i2 and i4, respectively, showed matching behavior of an IMPLY gate (Figure 1d and Figure S2) truth table.

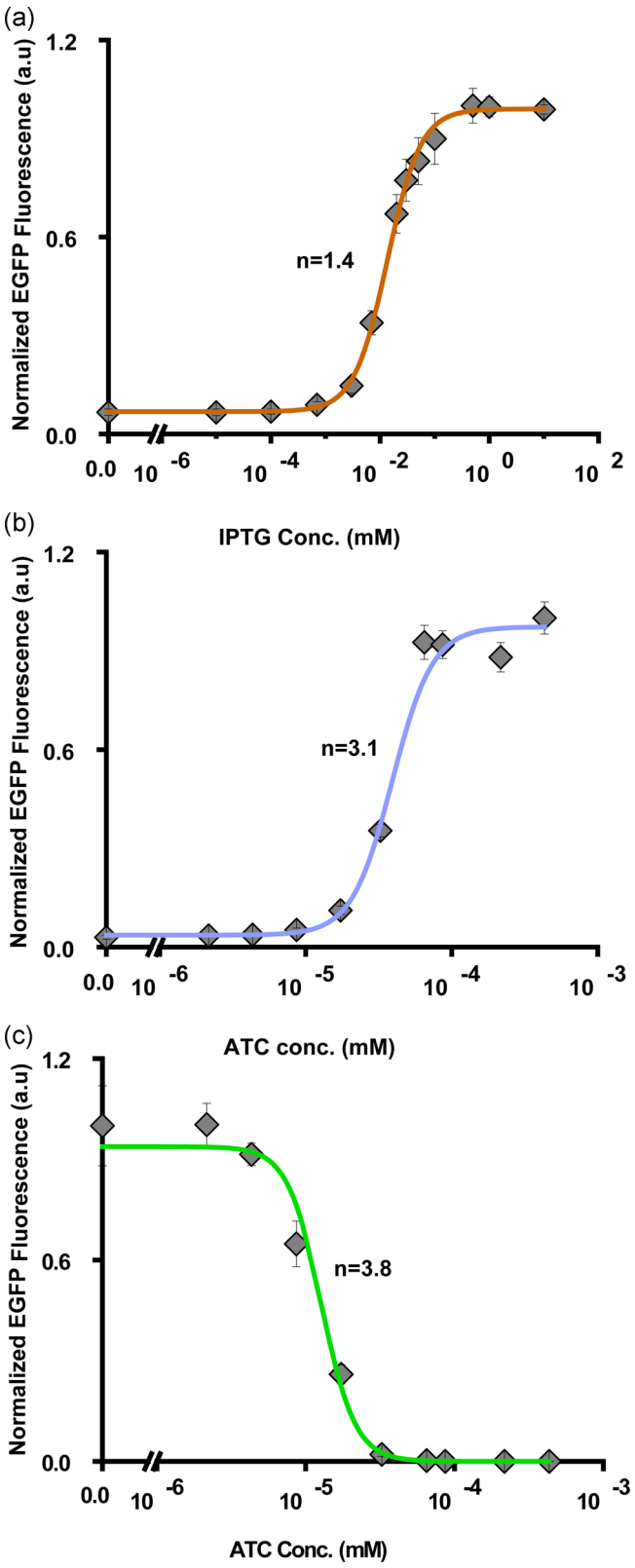

3.4 | Mathematical modeling, digitality, simulation, and experimental validation of IMPLY device

A genetic device should ideally be mathematically predictable and digital in its response. To demonstrate such device physics in our systems, we developed a simple ordinary differential equation (ODE)-based kinetic model (see Note S1 for details) to capture the input-output relation for the IMPLY gate. The model was based on a phenomenological Hill function (Equations 1 and 2), which was applied to explain genetic circuits (Roquet & Lu, 2014). The numerical values of the Hill coefficient "n_i" estimate the degree of sensitivity of the "output" as a function of "input." For "ni" greater than 1, the gene circuit is conventionally considered as digital-like or ultrasensitive (Roquet & Lu, 2014). Here, the EGFP expression (output) as a function of two inputs (IPTG and ATC) of the IMPLY gate was modeled through Equation 1.

$$\frac{d[EGFP]}{dt} = k_a\left[\left(b_1 + \frac{\left(\frac{[IPTG]}{K_1}\right)^{n_1}}{1+\left(\frac{[IPTG]}{K_1}\right)^{n_1}}\right)\left(b_2 + \frac{\left(\frac{[ATC]}{K_2}\right)^{n_2}}{1+\left(\frac{[ATC]}{K_2}\right)^{n_2}}\right) + \left(b_3 + \frac{1}{1+\left(\frac{[ATC]}{K_3}\right)^{n_3}}\right)\right] - k_d[EGFP], \quad (1)$$

$$[EGFP]_{ss} = c\left(b_1 + \frac{\left(\frac{[IPTG]}{K_1}\right)^{n_1}}{1+\left(\frac{[IPTG]}{K_1}\right)^{n_1}}\right)\left(b_2 + \frac{\left(\frac{[ATC]}{K_2}\right)^{n_2}}{1+\left(\frac{[ATC]}{K_2}\right)^{n_2}}\right) + c\left(b_3 + \frac{1}{1+\left(\frac{[ATC]}{K_3}\right)^{n_3}}\right), \quad (2)$$

FIGURE 3 (a and b) Dose-response curves for module 1 (P_{LTATAA} –EGFP in DH5αZ1), where for (a) anhydrotetracycline (ATC) concentration was kept constant at its saturated concentration 200 ng/ml and for (b) isopropyl β-D-1-thiogalactopyranoside (IPTG) concentration was kept constant at its saturated concentration, 10 mM. (c) Dose-response curve of module 2 (Plteto_1-CIm, P_R-EGFP in DH5αZ1). The "n" signifies the Hill coefficient for corresponding dose-response curves [Color figure can be viewed at wileyonlinelibrary.com]

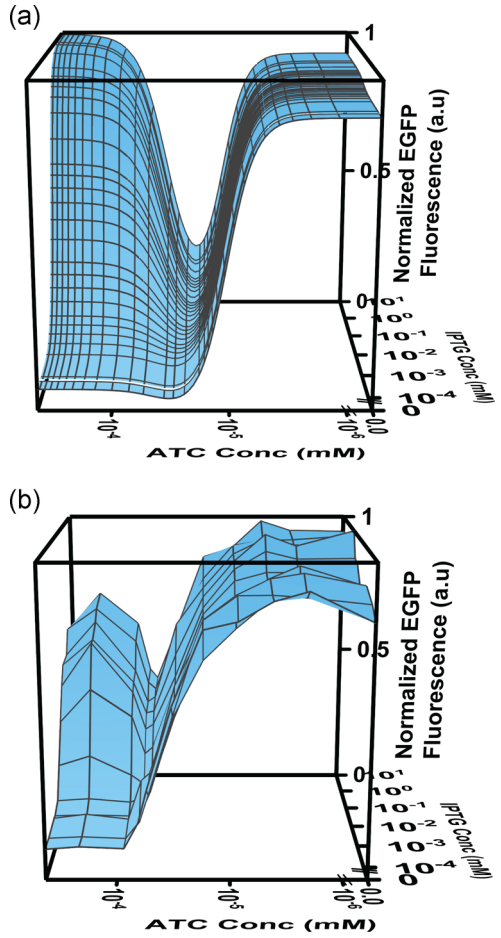

FIGURE 4 Simulated (a) and experimental (132 data points) (b) behavior of IMPLY gate [Color figure can be viewed at wileyonlinelibrary.com]

where k_a is scaling constant, *Ki* is Hill constant, *ni* is hill coefficient, *bi* denotes basal level expression, and *c* is equal to (k_a/k_d).

Equation 2 is additive and represents the behavior of two distinct molecular genetic modules, module 1 (P_{LTATAA} –EGFP in DH5αZ1) and module 2 (Plteto_1-CIm, P_R-EGFP in DH5αZ1), respectively. We assumed that this additive property held well in actual molecular circuits inside the cell. Therefore, we inserted module 1 and module 2 separately in *E. coli* and experimentally characterize their dose-response curves as a function of inducers (IPTG and ATC) concentration, keeping one of them constant at the saturated concentration (Figure 3).

We then fitted the dose-response behavior with the appropriate reduced form of Equation 2 (see Note S1 for details) separately and extracted the numerical parameters (Table S6). The Hill coefficient values (1.4, 3.1, and 3.8) suggested digital-like response behavior with respect to intensity (concentration) of the environmental chemical signals. Plugging the parameter values in Equation 2, we computationally simulate the input-output behavior of the whole IMPLY gate. Figure 4 shows the results. The simulated results are shown in Figure 4a. We performed another set of experiments to verify if the simulated results matched with the experiments. Figure 4b shows the experimental results, which suggest a close match with the simulation. However, though this Hill type of modeling is good enough to capture the overall input-output relationship of a synthetic genetic circuit in ensemble experiments, it may not be useful to model at low number regime or single-cell level as it does not incorporate noise associated with the biochemical reactions.

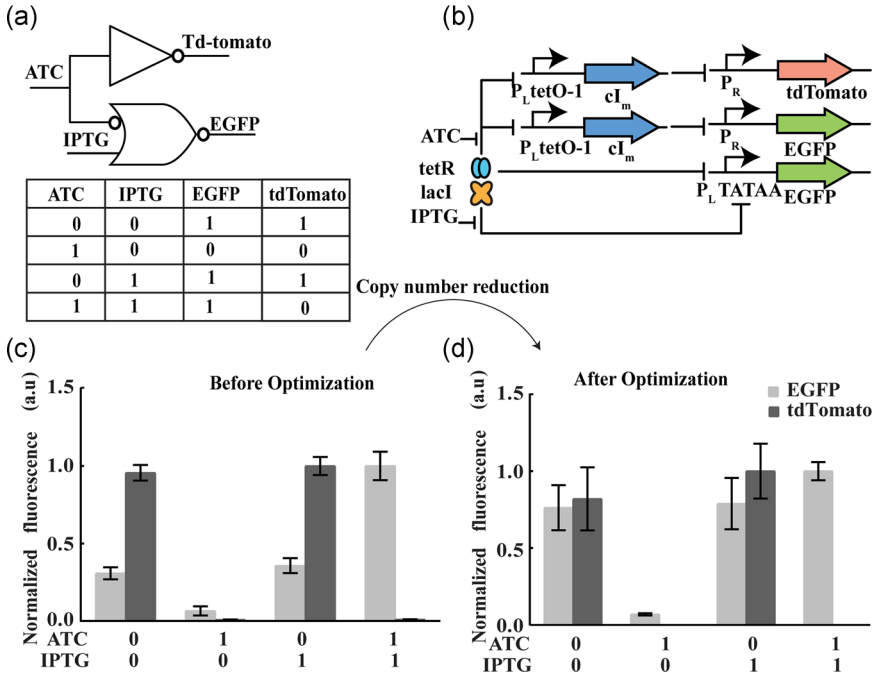

ATC	IPTG	EGFP	tdTomato
0	0	1	1
1	0	0	0
0	1	1	1
1	1	1	0

FIGURE 5 Design and testing of 2-input-2-output integrated logic circuit. (a) Electronic equivalent representation and truth table. (b) Biomolecular design. (c) Experimental behavior before optimization and (d) experimental behavior after optimization [Color figure can be viewed at wileyonlinelibrary.com]

3.5 | Higher-level signal decoding with a 2-input-2-output integrated circuit that integrates IMPLY and a NOT gate

To test if the chemical signal processing by IMPLY gate could work as a part of a larger signal processing device within a single cell and to create a device out of IMPLY with higher signal differentiation capability, we created a 2-input-2-output integrated circuit by connecting a NOT gate with the input line of the IMPLY gate (Figure 5). Although IMPLY is a powerful constraint-based logic, in terms of decoding, it can only differentiate between 1,0 and 00/01/11 input states by showing 0 and 1 logic output, respectively. The NOT gate sensed environmental ATC and responded inversely by producing EGFP. We constructed this NOT gate by placing a *TdTomato* gene (produce an orange fluorescent protein) under P_R promoter, which can be repressed by CIm protein coming from an ATC/TetR inducible PltetO-1 promoter. This NOT gate was integrated with the IMPLY gate (Figure 5a,b). The integrated circuit consisted of five genetic cassettes (Table S1) in a single plasmid and a total of seven genes were required for the functionality of the circuit. However, the experimental behavior of the first construct did not match with the truth table (Figure 5c).

It was reasoned that as the molecular circuits inside cells did not have any insulation, the leakage of CIm (basal level expression) from the NOT gate PltetO-1 promoter added up with the leakage from PltetO-1 promoter of module 2 of IMPLY gate and increased the cellular availability of CIm protein, which resulted in the partial repression of the EGFP expression from the P_R promoter. Therefore, a difference in output EGFP expression levels between synthetic P_{LTAAT} and P_R promoter was observed.

To reduce the CIm concentration, the number of available plasmids in the cell was reduced by changing the origin of replication from ColE1 (high copy) to p15A (low copy; Lutz & Bujard, 1997). The optimized circuit showed matching behavior with the truth table (Figure 5d). The 2-input-2-output integrated circuit sensed both the extracellular chemicals, IPTG and ATC, however, it was able to differentiate a higher number of input states combination (11, 10, and 00/01) than that of IMPLY gate alone.

We also developed a mathematical model for this integrated logic circuit. The integrated circuit consists of IMPLY gate expressing EGFP and a NOT gate expressing *tdTomato*. The overall behavior of the integrated circuit can be explained by following two ODEs (Equations 3 and 4),

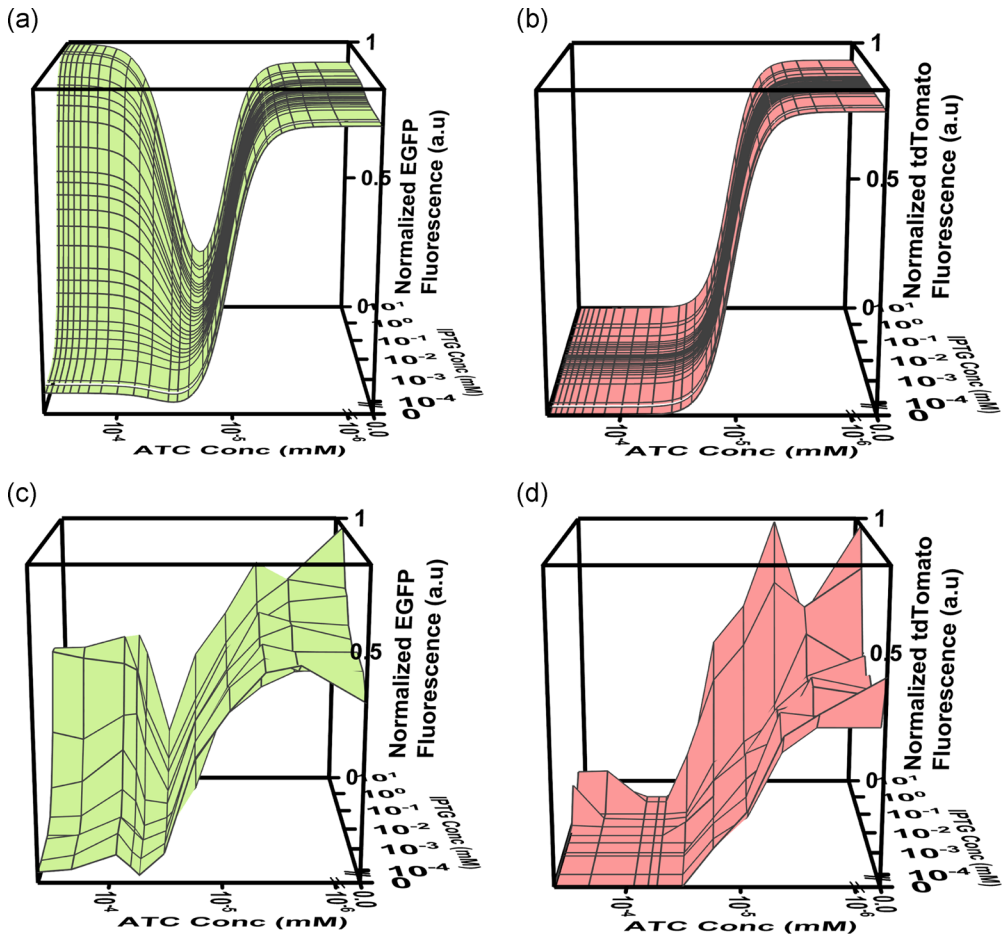

FIGURE 6 Simulated and experimental behavior of 2-input-2-output integrated logic circuit. Simulated behavior of (a) output 1 (enhanced green fluorescent protein [EGFP]) and (b) output 2 (*TdTomato*). Experimental behavior (121 data points each) of (c) output 1 (EGFP) and (d) output 2 (*TdTomato*) as a function of two input chemicals in the full integrated circuit inside cell [Color figure can be viewed at wileyonlinelibrary.com]

$$\frac{d[EGFP]}{dt} = k'_a\left[\left(b'_1 + \frac{\left(\frac{[IPTG]}{K'_1}\right)^{n'_1}}{1+\left(\frac{[IPTG]}{K'_1}\right)^{n'_1}}\right)\left(b'_2 + \frac{\left(\frac{[ATC]}{K'_2}\right)^{n'_2}}{1+\left(\frac{[ATC]}{K'_2}\right)^{n'_2}}\right) + \left(b'_3 + \frac{1}{1+\left(\frac{[ATC]}{K'_3}\right)^{n'_3}}\right)\right] - k'_d[EGFP], \quad (3)$$

$$\frac{d[tdTomato]}{dt} = k''_a\left(b_4 + \frac{1}{1+\left(\frac{[ATC]}{K_4}\right)^{n4}}\right) - k''_d[tdTomato], \quad (4)$$

where the notations represent the usual meaning as in Equation 1. Assuming the hierarchical principle of electronics held well in in-cell systems chemistry, we created reduced forms of the equations based on an individual set of molecular modules, fitted with experimental data to estimate the parameters (Note S1). We further simulated the input-output behavior for this integrated circuit and Figure 6 shows a close topological match between simulation and experiments. We believed that the little discrepancies observed between the model and the experiment arose from the assumption of unaltered behavior of molecular modules within an integrated circuit. The hierarchy principle in in-cell molecular computation is challenging due to the crosstalk of DNA modules and background cellular context (Falk, Bronstein, Hanst, Drossel, & Koeppl, 2019). Both the IMPLY and integrated circuit were designed and fabricated assembling module

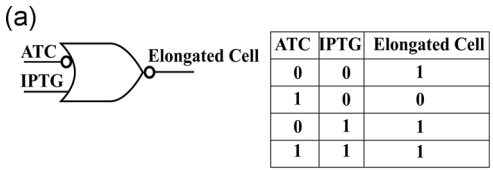

ATC	IPTG	Elongated Cell
0	0	1
1	0	0
0	1	1
1	1	1

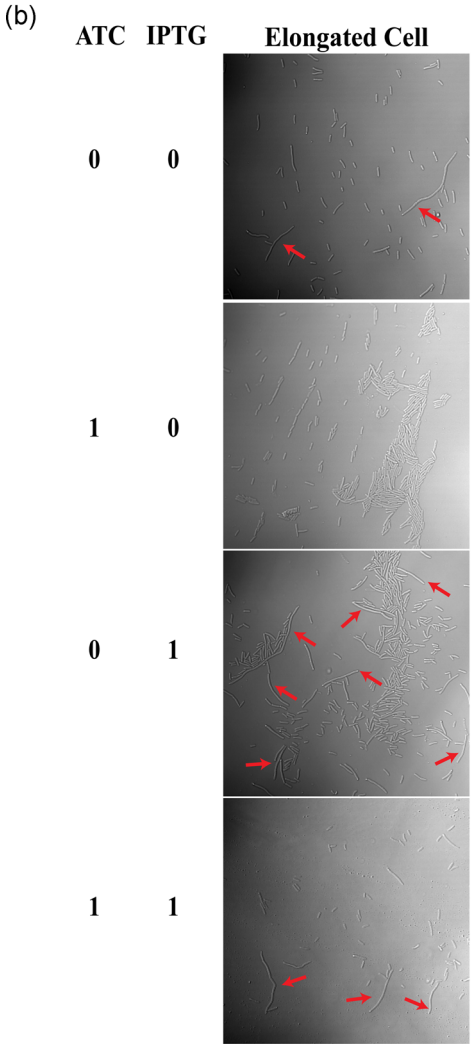

FIGURE 7 (a) The IMPLY circuit with phenotypic output. (b) Experimental behavior of the engineered cell. The red arrows are pointing towards elongated cells [Color figure can be viewed at wileyonlinelibrary.com]

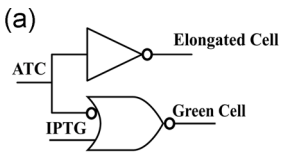

ATC	IPTG	Green Cell	Elongated Cell
0	0	1	1
1	0	0	0
0	1	1	1
1	1	1	0

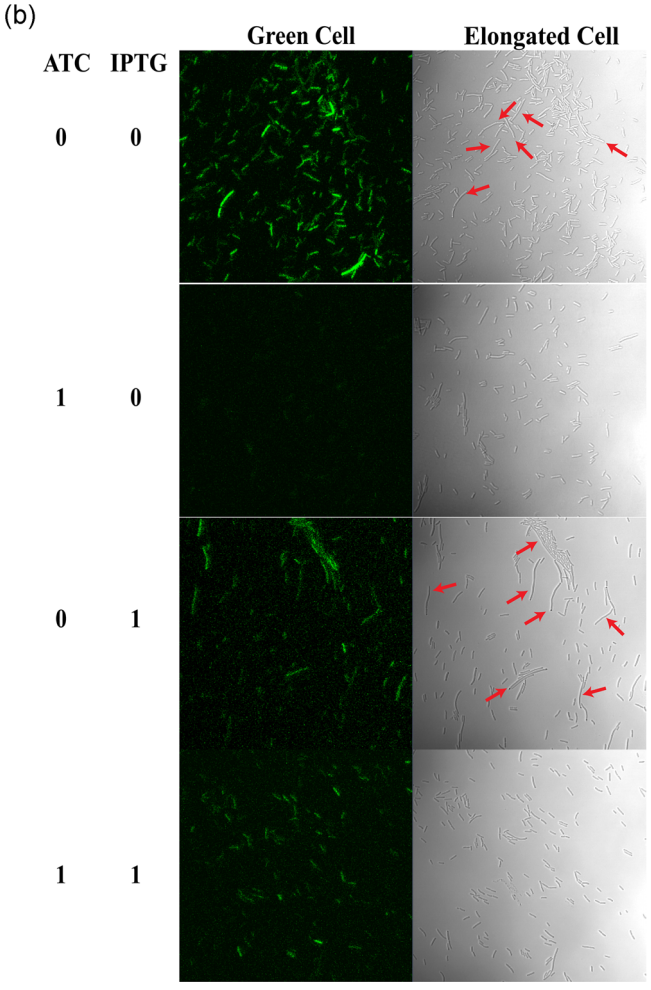

FIGURE 8 (a) The 2-input-2-output circuit with phenotypic outputs. (b) Experimental behavior of the engineered cell. The red arrows are pointing towards elongated cells [Color figure can be viewed at wileyonlinelibrary.com]

by module. Similarly, the mathematical model was constructed by summing up the equations represent the modules. This suggested the successful application of the hierarchy principle of electronics in terms of abstraction, decoupling, and standardization at the level of in-cell systems chemistry (Andrianantoandro et al., 2006).

3.6 | Integration of the circuits with native cellular process

Next, to show a simple application, we integrated this IMPLY (Figure 7) and 2-input-2-output circuit (Figure 8) with inherent cellular process. ftsZ is a native protein, which helps in cell division in *E. coli* (Sánchez-Gorostiaga et al., 2016). Deregulation of ftsZ results a nondivided, elongated shaped *E. coli*. Here we used a synthetic small regulatory RNA (synRNA) against the ftsZ messenger RNA (mRNA; Mukhopadhyay & Bagh, 2019, Table S3). SynRNA can be designed to control the expression of target protein by binding with the target mRNA to hinder its translation (Yoo, Na, & Lee, 2013). We replaced the EGFP with anti-ftsZ synRNA of the IMPLY gate, such that the new IMPLY gate had a phenotypic output (elongated cell shape; Figure 7a). The experimental characterization of the engineered cell showed a matching behavior with the expected IMPLIES truth table (Figure 7b).

In the second construct, we replaced the *tdTomato* gene of the 2-input-2-output circuit with the anti-ftsZ synRNA to create a new circuit, which had two phenotypic outputs, namely "elongated shape" (resulted from anti- ftsZ synRNA) and "green colour" (resulted from EGFP expression; Figure 8a). Experimental characterization with the engineered cells showed matching behavior with the corresponding truth table (Figure 8b).

4 | CONCLUSION

In conclusion, we created a fully and chemically controllable in-cell molecular genetic IMPLY gate in a single *E. coli*, which can sense, integrate, and process two extracellular environmental chemical signals. This adds constraint-based fundamental logic in the in-cell molecular computation and completes the toolbox. Our design is generic and can be used to create other IMPLY gates with other equivalent inducers and repressor interactions. The successful function of IMPLY gate within a 2-input-2-output integrated circuit, suggests its ability as a part of a larger circuit. The 2-input-2-output integrated circuit, due to its higher differentiation capability between combinations of input signals, has significance as a cell-based chemical signal-decoding device. As the output genes of IMPLY and the 2-input-2-output circuits can be changed to any genes, this could be useful to control cellular or metabolic pathways in *E. coli* from outside, in a specific logical manner. In the 2-input-2-output circuit, which was made from the IMPLY gate, it is possible to reverse the expression of the *tdTomato* gene more than once by "adding" inducers sequentially to the system (Figure 5d). This property could be useful to control the ON and OFF of a gene multiple times just by adding the inducers in sequence, instead of flushing out the inducers from the system. This property can be very useful to control a cellular or metabolic process in a running reactor, where it is not convenient to flush out any inducer from the media during the run to reverse the expression of a gene. Due to the significance of constraint-based logic in robotics and control, the constraint-based genetic IMPLY may have significance in the future development of microbiorobotics and chemical control. Further, as the IMPLY gate and the combinatorial circuit made from it were implemented in a single cell, in fact in a single plasmid, the design may be applied to control intracellular process in a specific logical manner by changing its output proteins as shown in Figures 7 and 8. Such intracellular IF-THEN logic may be applied to control other metabolic and cellular processes in future, which cannot be achieved by multicellular implementation (Tamsir et al., 2011).

The function of those circuits is digital-like and mathematically predictive. The modules and their integration in both experiments and models suggested the successful application of the electronic hierarchy principle in in-cell molecular circuitry. This may serve as a general design criterion in creating future complex whole-cell smart biosensing and signal processing devices. To fabricate and optimize the signal processing circuits, we developed a new process pipeline, which allowed fast parallel optimizations of rate parameters of gene expression, eliminated unwanted kinetic influence from one DNA module to the other, and overcome the limitation of previous methods. This pipeline can be useful for systematic fabrication and fast optimization of large and complex DNA-based molecular circuits. Taken together, this study has implications in in-cell complex molecular computation, smart whole-cell biosensors, signal-decoding device, microbiorobotics, and synthetic biology.

ACKNOWLEDGMENTS

This study was mostly supported by SINP Intramural Funding, Department of Atomic Energy, Govt. of India, and partially funded by Ramanujan Fellowship of SB, Department of Science and Technology, Govt. of India and Synthetic Biology Program, Biotechnology Industry Research Assistance Council (BIRAC), Govt. of India.

CONFLICT OF INTERESTS

The authors declare that there are no conflict of interests.

ORCID

Sangram Bagh http://orcid.org/0000-0002-8565-0728

REFERENCES

Anderson, J. C., Voigt, C. A., & Arkin, A. P. (2007). Environmental signal integration by a modular AND gate. *Molecular Systems Biology*, *3*, 133. https://doi.org/10.1038/msb4100173

Andrianantoandro, E., Basu, S., Karig, D. K., & Weiss, R. (2006). Synthetic biology: New engineering rules for an emerging discipline. *Molecular Systems Biology*, *2*, 2006.0028. https://doi.org/10.1038/msb4100073

Ashkenasy, G., Hermans, T. M., Otto, S., & Taylor, A. F. (2017). Systems chemistry. *Chemical Society Reviews*, *46*, 2543–2554. https://doi.org/10.1039/C7CS00117G

Ausländer, S., Ausländer, D., Müller, M., Wieland, M., & Fussenegger, M. (2012). Programmable single-cell mammalian biocomputers. *Nature*, *487*, 123–127.

Bonnet, J., Yin, P., Ortiz, M. E., Subsoontorn, P., & Endy, D. (2013). Amplifying genetic logic gates. *Science*, *340*(6132), 599–603. https://doi.org/10.1126/science.1232758

Borghetti, J., Snider, G. S., Kuekes, P. J., Yang, J. J., Stewart, D. R., & Williams, R. S. (2010). 'Memristive' switches enable 'stateful' logic operations via material implication. *Nature*, *464*, 873–876.

Cameron, D. E., Bashor, C. J., & Collins, J. J. (2014). A brief history of synthetic biology. *Nature Reviews Microbiology*, *12*, 381–390. https://doi.org/10.1038/nrmicro3239

Castelfranchi, C., & Lespéran, Y., 2001. Intelligent agents VII: agent theories architectures and languages: 7th International Workshop, ATAL 2000, Boston, MA, July 7–9, 2000: proceedings, Proceedings of the 7th International Workshop on Intelligent Agents VII. Agent Theories Architectures and Languages. Springer.

Che, A., 2004. BioBricks++: Simplifying Assembly of Standard DNA Components.

Chen, Y. J., Liu, P., Nielsen, A. A. K., Brophy, J. A. N., Clancy, K., Peterson, T., & Voigt, C. A. (2013). Characterization of 582 natural and synthetic terminators and quantification of their design constraints. *Nature Methods*, *10*, 659–664. https://doi.org/10.1038/nmeth.2515

Espah Borujeni, A., Channarasappa, A. S., & Salis, H. M. (2014). Translation rate is controlled by coupled trade-offs between site accessibility, selective RNA unfolding and sliding at upstream standby sites. *Nucleic Acids Research*, *42*, 2646–2659. https://doi.org/10.1093/nar/gkt1139

Falk, J., Bronstein, L., Hanst, M., Drossel, B., & Koeppl, H. (2019). Context in synthetic biology: Memory effects of environments with mono-molecular reactions. *Journal of Chemical Physics*, *150*, 024106. https://doi.org/10.1063/1.5053816

Fink, T. L., Klepcyk, P. J., Oette, S. M., Gedeon, C. R., Hyatt, S. L., Kowalczyk, T. H., … Cooper, M. J. (2006). Plasmid size up to 20kbp does not limit effective in vivo lung gene transfer using compacted DNA nanoparticles. *Gene Therapy*, *13*, 1048–1051. https://doi.org/10.1038/sj.gt.3302761

Goñi-Moreno, A., & Nikel, P. I. (2019). High-performance biocomputing in synthetic biology–integrated transcriptional and metabolic circuits. *Frontiers in Bioengineering and Biotechnology*, *7*, 40. https://doi.org/10.3389/fbioe.2019.00040

Green, A. A., Kim, J., Ma, D., Silver, P. A., Collins, J. J., & Yin, P. (2017). Complex cellular logic computation using ribocomputing devices. *Nature*, *548*, 117–121.

Guet, C. C., Elowitz, M. B., Hsing, W., & Leibler, S. (2002). Combinatorial synthesis of genetic networks. *Science*, *296*, 1466–1470. https://doi.org/10.1126/science.1067407

Jusiak, B., Cleto, S., Perez-Piñera, P., & Lu, T. K. (2016). Engineering synthetic gene circuits in living cells with CRISPR technology. *Trends in Biotechnology*, *34*, 535–547. https://doi.org/10.1016/j.tibtech.2015.12.014

Kampis, J. (1991). *Self Modifying Systems in Biology and Cognitive Science, IFSR International Series on Systems Science and Engineering* (p. 271). Oxford, UK: Pergamon Press.

Kim, M., Steager, E., & Agung, J. (2012). *Microbiorobotics: biologically inspired microscale robotic systems*. Waltham, USA: Elsevier.

Lutz, R., & Bujard, H. (1997). Independent and tight regulation of transcriptional units in *Escherichia Coli* via the LacR/O, the TetR/O and AraC/I1-I2 regulatory elements. *Nucleic Acids Research*, *25*, 1203–1210. https://doi.org/10.1093/NAR/25.6.1203

Moon, T. S., Lou, C., Tamsir, A., Stanton, B. C., & Voigt, C. A. (2012). Genetic programs constructed from layered logic gates in single cells. *Nature*, *491*, 249–253.

Mukhopadhyay, S., & Bagh, S. 2019. A synthetic genetic microgravity sensor (unpublished results, submitted manuscript).

Nomura, Y., & Yokobayashi, Y. (2015). In L. Ponchon (Ed.), *Aptazyme-Based Riboswitches and Logic Gates in Mammalian Cells BT - RNA Scaffolds: Methods and Protocols* (pp. 141–148). New York, NY: Springer New York. https://doi.org/10.1007/978-1-4939-2730-2_12

Phillips, I., & Silver, P., 2006. A New Biobrick Assembly Strategy Designed for Facile Protein Engineering.

Roquet, N., & Lu, T. K. (2014). Digital and analog gene circuits for biotechnology. *Biotechnology Journal*, *9*, 597–608.

Russell, B., & Whitehead, A. N. (1910). *Principia Mathematica 1*. Cambridge: Cambridge University Press.

Salis, H. M., Mirsky, E. A., & Voigt, C. A. (2009). Automated design of synthetic ribosome binding sites to control protein expression. *Nature Biotechnology*, *27*, 946–950. https://doi.org/10.1038/nbt.1568

Sarkar, K., Mukhopadhyay, S., Bonnerjee, D., Srivastava, R., & Bagh, S. (2019). A frame-shifted gene, which rescued its function by non-natural start codons and its application in constructing synthetic gene circuits. *Journal of Biological Engineering*, *13*, 20. https://doi.org/10.1186/s13036-019-0151-x

Shetty, R. P., Endy, D., & Knight, T. F., Jr (2008). Engineering BioBrick vectors from BioBrick parts. *Journal of Biological Engineering*, *2*, 5. https://doi.org/10.1186/1754-1611-2-5

Siuti, P., Yazbek, J., & Lu, T. K. (2013). Synthetic circuits integrating logic and memory in living cells. *Nature Biotechnology*, *31*, 448–452.

Swart, de, H. C. M., & Nederpelt, R. P. (1992). Implication: A survey of the different logical analyses of 'if…, then…'. *Nieuw Archief voor Wiskunde*, *4/10*(1-2), 77–104.

Sánchez-Gorostiaga, A., Palacios, P., Martínez-Arteaga, R., Sánchez, M., Casanova, M., & Vicente, M. (2016). Life without division: Physiology of *Escherichia Coli* FtsZ-deprived filaments. *mBio*, *7*(5), e01620-16. https://doi.org/10.1128/mBio.01620-16

Tamsir, A., Tabor, J. J., & Voigt, C. A. (2011). Robust multicellular computing using genetically encoded NOR gates and chemical 'wires'. *Nature*, *469*, 212–215.

Weiss, R., & Basu, S., 2002. The Device Physics of Cellular Logic Gates, First Workshop on Non-Silicon Computing, Cambridge, MA.

Yokobayashi, Y., Weiss, R., & Arnold, F. H. (2002). Directed evolution of a genetic circuit. *Proceedings of the National Academy of Sciences of the United States of America*, *99*, 16587–16591. https://doi.org/10.1073/pnas.252535999

Yoo, S. M., Na, D., & Lee, S. Y. (2013). Design and use of synthetic regulatory small RNAs to control gene expression in *Escherichia Coli*. *Nature Protocols*, *8*, 1694–1707.

SUPPORTING INFORMATION

Additional supporting information may be found online in the Supporting Information section.

How to cite this article: Mukhopadhyay S, Sarkar K, Srivastava R, Pal A, Bagh S. Processing two environmental chemical signals with a synthetic genetic IMPLY gate, a 2-input-2-output integrated logic circuit, and a process pipeline to optimize its systems chemistry in *Escherichia coli*. *Biotechnology and Bioengineering*. 2020;117:1502–1512. https://doi.org/10.1002/bit.27286